Materials Advances

ROYAL SOCIETY OF CHEMISTRY

PAPER

View Article Online
View Journal | View Issue

Cite this: *Mater. Adv.*, 2023, 4, 2099

Changes in permselectivity of radiation-grafted anion-exchange membranes with different cationic headgroup chemistries are primarily due to water content differences†

Arup Chakraborty, Ihtasham Salam, Mehdi Choolaei, Judy Lee, Carol Crean, Daniel K. Whelligan, Rachida Bance-Soualhi and John R. Varcoe *

In a prior paper [Bance-Soualhi *et al.*, *J. Mater. Chem. A*, 2021, **9**, 22025], we showed that the crosslinking of radiation-grafted anion-exchange membranes (RG-AEM) was necessary to obtain high enough apparent permselectivities for use in applications such as (reverse)electrodialysis. However, a separate result in this prior study suggested that comparable AEMs (similar ion-exchange capacity, IEC, and backbone chemistry) with different cationic headgroups may yield different balances between permselectivity and conductivity. This short follow-up study compares the permselectivities and Cl^- conductivities of a series of non-crosslinked RG-AEMs with either aliphatic quaternary ammonium headgroups (*N*-benzyl-*N*-methylpiperidinium, MPIP, and benzyltrimethylammonium, TMA) or aromatic cationic headgroups (*N*-benzylpyridinium, PYR, or 1-benzyl-2,3-dimethylimidazolium, DMI). We show that a change in the headgroup chemistry modified the permselectivity-conductivity balance of the RG-AEM, but this was primarily due to the different headgroups inducing varying intrinsic water contents: higher water content RG-AEMs yield lower permselectivites. As also expected from this water content observation, higher IEC variants yielded RG-AEMs with lower permselectivities. The addition of *N*,*N*,*N*′,*N*′-tetramethylhexane-1,6-diamine-(TMHDA)-based ionic crosslinking to a DMI-based RG-AEM also raised permselectivity, confirming the observation of the prior study also applies to aromatic headgroup RG-AEMs. In summary, high IEC AEMs containing imidazolium-type headgroups along with an optimal amount of ionic crosslinking could be promising and warrant more study (*i.e.* a comparison of RG-AEMs with cheaper, more scalable non-RG-analogues that contain these attributes).

Received 21st February 2023,
Accepted 31st March 2023

DOI: 10.1039/d3ma00082f

rsc.li/materials-advances

Introduction and context

The optimal balance between the permselectivity and conductivity of ion-exchange membranes (IEM) is important for their successful deployment in applications such as reverse electrodialysis (RED).[1] It is desirable to deploy an IEM that has both a high permselectivity and a high conductivity (low *in situ* ohmic resistance).[2] This paper reports a short follow-up to a prior 2021 study that looked into the most effective method of crosslinking radiation-grafted anion-exchange membranes (RG-AEM) in order to raise permselectivies whilst avoiding excessive reductions in conductivity.[3] The key findings from this prior paper were:

1. Non-crosslinked RG-AEMs containing aliphatic quaternary ammonium (positively charged, cationic) headgroups exhibited low permselectivities;

2. The addition of crosslinking led to raised permselectivies at the expense of raised ohmic resistances (reduced conductivities);

3. Crosslinking using divinylbenzene (DVB) in the grafting step of RG-AEM fabrication (yielding rigid, non-ionic crosslinks) led to improvements in permselectivity but with excessively raised resistances;

4. Crosslinking using *N*,*N*,*N*′,*N*′-tetramethylhexane-1,6-diamine (TMHDA) in the amination step of RG-AEM fabrication (yielding more flexible ionic crosslinks) led to lower increases in resistance for comparable improvements in permselectivity (*cf.* DVB crosslinking);

It was also observed that a non-crosslinked RG-AEM containing the *N*-benzyl-*N*-methylpiperidinium (MPIP) headgroup exhibited a different permselectivity-conductivity property balance compared to a non-crosslinked RG-AEM containing the more widely reported benzyltrimethylammonium (TMA) headgroup chemistry.

This study builds up from the latter observation and addresses the question: does the cationic headgroup chemistry of an RG-AEM intrinsically affect the balance of permselectivity

School of Chemistry and Chemical Engineering, The University of Surrey, Guildford, GU2 7XH, UK. E-mail: j.varcoe@surrey.ac.uk

† Raw data (CC-BY) can be found at DOI: https://doi.org/10.6084/m9.figshare.22128719

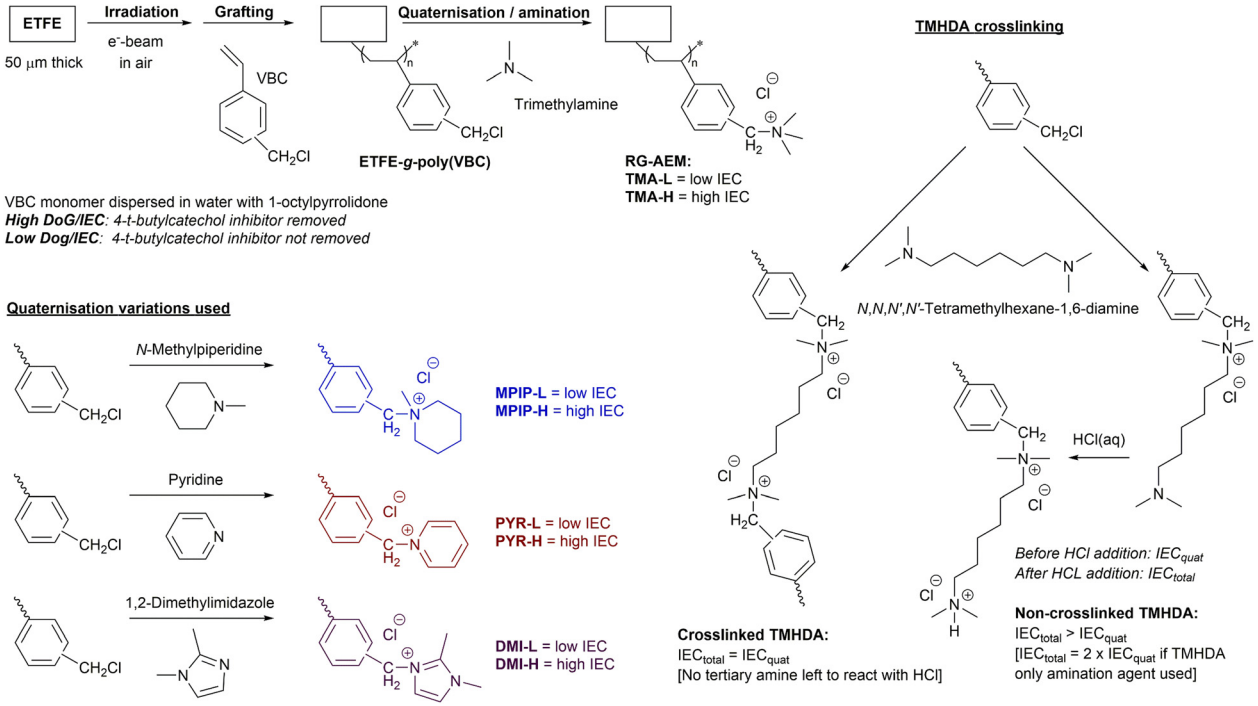

Scheme 1 The radiation-grafting of vinylbenzyl chloride (VBC) monomer onto ETFE films to form the ETFE-*g*-poly(VBC) intermediate membrane, with subsequent amination to yield the target radiation-grafted anion-exchange membranes (RG-AEMs) containing the following cationic headgroups: benzyltrimethylammonium chloride (TMA), *N*-benzyl-*N*-methylpiperidinium chloride (MPIP), *N*-benzylpyridinium (PYR), and 1-benzyl-2,3-dimethylimidazolium chloride (DMI). Both a high and a low IEC series of RG-AEMs were fabricated (designated X-H and X-L, respectively, where X = the cationic headgroup), as controlled by removal or retention of the 4-*tert*-butylcatechol polymerisation inhibitor in the supplied VBC monomer, respectively. The schematic to the right gives details of reaction of grafted poly(VBC) groups with *N*,*N*,*N*′,*N*′-tetramethylhexane-1,6-diamine (TMHDA), where IEC_{total} = IEC_{quat} confirms crosslinking (see ref. 3 for more details on the titration-based determination of IEC_{total} and IEC_{quat}). TMHDA was used to produce a high IEC, crosslinked DMI-based RG-AEM (designated DMI-TMHDA-H).

to conductivity (with comparable ion-exchange capacities, IEC)? This question was previously probed by Ji *et al.* using DVB-crosslinked polystyrenic-*co*-acrylonitrile AEMs containing two cationic headgroups:[4] benzyltrimethylammonium (TMA) or 1-benzyl-2,3-dimethylimidazolium (DMI). To further address this question, our study involved both a high IEC and a low IEC series of Cl^--form RG-AEMs that were fabricated with the following cationic headgroup chemistries (Scheme 1):

1. Aliphatic non-cyclic benzyltrimethylammonium (TMA);
2. Aliphatic heterocyclic *N*-benzyl-*N*-methylpiperidinium (MPIP);
3. Aromatic 1-N heterocyclic *N*-benzylpyridinium (PYR);
4. Aromatic 2-N heterocyclic 1-benzyl-2,3-dimethylimidazolium (DMI).

A high IEC RG-AEM with the best performing headgroup was then fabricated with additional TMHDA-crosslinking to verify the observations in the predecessor paper.[3]

Materials and methods

Materials and chemicals

RG-AEMs were prepared using the 50 μm thick ETFE film (Nowoflon ET-6235Z, Nowofol Kunstoffprodukte GmbH). Vinylbenzyl chloride monomer (VBC, Polysciences Europe GmbH, product code 02718-500, 96+% purity) was supplied as a mixture of *meta*- and *para*-isomers with an initial inhibitor concentration between 50–100 ppm 4-*tert*-butylcatechol. For removal of the inhibitor, the monomer was passed through a column packed with inhibitor removal powder (Merck Life Science UK, product code 311340-500G) following the instructions supplied. 1-Octyl-2-pyrrolidone (Merck Life Science UK) was used as dispersant without further purification. For quaternisation steps (Table 1), aqueous trimethylamine solution (45 wt%), *N*-methylpiperidine (99% purity), pyridine (PYR, anhydrous 99.8% purity), 1,2-dimethylimidazole (97% purity) and *N*,*N*,*N*′,*N*′-tetramethylhexene-1,6-diamine (TMHDA, 99% purity) were used without further purification (Merck Life Science UK). For Cl^- precipitation titrations for IEC determinations, aqueous $AgNO_3$ (0.0200 ± 0.0006 mol dm^{-3}, Honeywell) was used as the analytical titrant. All other chemicals, including analytical grade NaCl (99+% purity) for ion-exchange of the RG-AEMs to Cl^- form, $NaNO_3$ (extra pure, Fisher Scientific), aqueous HNO_3 (2 mol dm^{-3} volumetric solution, Fisher Scientific) and HCl (certified ACS Plus, 37 wt%) were used as received. Ultrapure water (UPW, resistivity = 18.2 MΩ cm) was used throughout this study.

Fabrication of the RG-AEMs (summarised in Scheme 1).

The core methods used to fabricate the intermediate VBC-grafted ETFE membrane (ETFE-*g*-poly(VBC)) were those detailed in the predecessor paper[3] with the following key modifications:

Table 1 The conditions used to convert the ETFE-*g*-poly(VBC) grafted membranes into the different chemistry RG-AEMs

RG-AEM designation	Quaternisation reagent	Reagent : UPW (vol. ratio)	Quaternisation temperature/°C	Quaternisation time/h
TMA-L and -H	Trimethylamine (aq, 45 wt%)	100 : 0	Room temperature (no heating)	24
MPIP-L and -H	*N*-Methylpiperidine (l)	15 : 85	80	24
PYR-L and -H	Pyridine (l)	15 : 85	80	24
DMI-L and -H	1,2-Dimethylimidazole (l)[a]	100 : 0	80	72

RG-AEM designation	Quaternisation reagent	TMHDA : Reagent : UPW (vol. ratio)	Quaternisation temperature/°C	Quaternisation time/h
DMI-TMHDA-H	1,2-Dimethylimidazole (l)[a]	5 : 95 : 0	80	72

[a] The solid 1,2-dimethylimidazole was melted before being reacted.

1. The as purchased ETFE films (15 cm × 15 cm) were subject to an e^--beam in ambient air to a total dose of 40 kGy with 10 kGy dose per pass (10 MeV beam, Sterigenics, Espergaerde, Denmark), after which the samples were immediately packed into dry ice and transported back to University of Surrey to be stored in a −40 °C freezer within 2 d of the e^--beam date;

2. The e^--beamed ETFE films were grafted with N_2 purged aqueous dispersions containing VBC (5 vol%) and 1-octyl-2-pyrrolidone (1 vol%) at 70 °C for 24 h. For the low degree of grafting (DoG) series (to make the low IEC RG-AEMs), the VBC was used as received, whereas for the high DoG series (to make the high IEC RG-AEMs), the inhibitor was removed from the VBC before grafting;

3. The resulting grafted ETFE-*g*-poly(VBC) membranes were thoroughly washed using acetone and kept in a vacuum oven overnight at 70 °C before subsequent quaternisation. The DoG values for the ETFE-*g*-poly(VBC) intermediate membranes used in this study are given in Table 2.

To form the various RG-AEMs, the ETFE-*g*-poly(VBC) membranes were quaternised using the conditions given in Table 1. The resulting RG-AEMs were washed with UPW and then kept in UPW for another 8 h at 70 °C to remove excess quaternisation reagents. To ensure the Cl^- forms, the RG-AEMs were immersed in a large excess aqueous NaCl (1 mol dm^{-3}) solutions in polypropylene vessels for 24 h, after which they were washed several times in UPW over 24 h to remove excess co-ions (Na^+) and counter-ions (Cl^-). The final pristine Cl^- form RG-AEMs were then stored in fresh UPW until required for further experiments.

Raman characterisation

Raman spectroscopy was used to confirm the formation, *via* quaternisation of the ETFE-*g*-poly(VBC) membrane, of the RG-desired AEMs with the different headgroup chemistries. Different cationic headgroups in RG-AEMs have highly diagnostic bands.[3,5–8] The spectra were recorded on a Renishaw InVia

Table 2 Key *ex situ* properties[3,7] of the Cl^--form RG-AEMs made from ETFE-*g*-poly(VBC) grafted intermediates of different degrees of grafting (DoG). Errors are sample standard deviations (n = 3 samples of each RG-AEMs) unless otherwise indicated. All measurements were conducted at room temperature unless otherwise indicated

High IEC series	TMA-H	MPIP-H	PYR-H	DMI-H	DMI-TMHDA-H
Degree of grafting, DoG (%)	110 ± 1				106 ± 1
IEC_{quat}/mmol g^{-1}	2.23 ± 0.04	2.03 ± 0.01	2.13 ± 0.04	2.13 ± 0.03	1.90 ± 0.07
IEC_{total}/mmol g^{-1}	—	—	—	—	2.08 ± 0.05
Thickness (dehydrated)/μm	88 ± 2[a]	84 ± 2[a]	80 ± 2[a]	85 ± 2[a]	96 ± 2[a]
Thickness (hydrated)/μm	117 ± 2[a]	117 ± 2[a]	109 ± 2[a]	110 ± 2[a]	100 ± 3[a]
Thickness swelling, TPS (%)	33 ± 3[b]	39 ± 4[b]	36 ± 4[b]	29 ± 3[b]	4 ± 4[b]
Water uptake, WU (%)	97 ± 1	129 ± 1	98 ± 2	77 ± 3	50 ± 2
$\lambda(H_2O)$	24 ± 1[b]	35 ± 1[b]	26 ± 1[b]	20 ± 1[b]	15 ± 1[b]
Apparent permselectivity, α (%)	48 ± 3[c]	41 ± 3[c]	48 ± 3[c]	57 ± 3[c]	83 ± 3[c]
Cl^- conductivity, σ/mS cm^{-1}[d]	23 ± 1[e]	17 ± 1[e]	24 ± 2[e]	24 ± 1[e]	15 ± 2[e]

Low IEC series	TMA-L	MPIP-L	PYR-L	DMI-L
Degree of grafting, DoG (%)	46 ± 1			
IEC_{quat}/mmol g^{-1}	1.58 ± 0.02	1.42 ± 0.02	1.47 ± 0.05	1.49 ± 0.01
Thickness (dehydrated)/μm	76 ± 3[a]	73 ± 2[a]	63 ± 2[a]	75 ± 4[a]
Thickness (hydrated)/μm	91 ± 2[a]	93 ± 2[a]	85 ± 2[a]	83 ± 2[a]
Thickness swelling, TPS (%)	20 ± 5[b]	27 ± 4[b]	35 ± 5[b]	11 ± 6[b]
Water uptake, WU (%)	42 ± 2	48 ± 2	47 ± 1	42 ± 2
$\lambda(H_2O)$	15 ± 1[b]	19 ± 1[b]	18 ± 1[b]	16 ± 1[b]
Apparent permselectivity, α (%)	67 ± 3[c]	64 ± 3[c]	60 ± 3[c]	68 ± 3[c]
Cl^- conductivity, σ/mS cm^{-1}[d]	14 ± 1[e]	10 ± 1[e]	19 ± 2[e]	14 ± 7[e]

[a] Errors are sample standard deviations from n = 3 measurements on each membrane or 2 μm (the minimum visual precision of the micrometer used), whichever is the greatest. [b] Errors are propagated uncertainties (calculated from the errors of input parameters). [c] Errors are larger than the measured sample standard deviations but are calculated assuming a ± 1 mV error in potential readings. [d] In-plane Cl^- conductivities in water at 25 °C. [e] Errors are sample standard deviations or 1 mS cm^{-1}, whichever is the greatest.

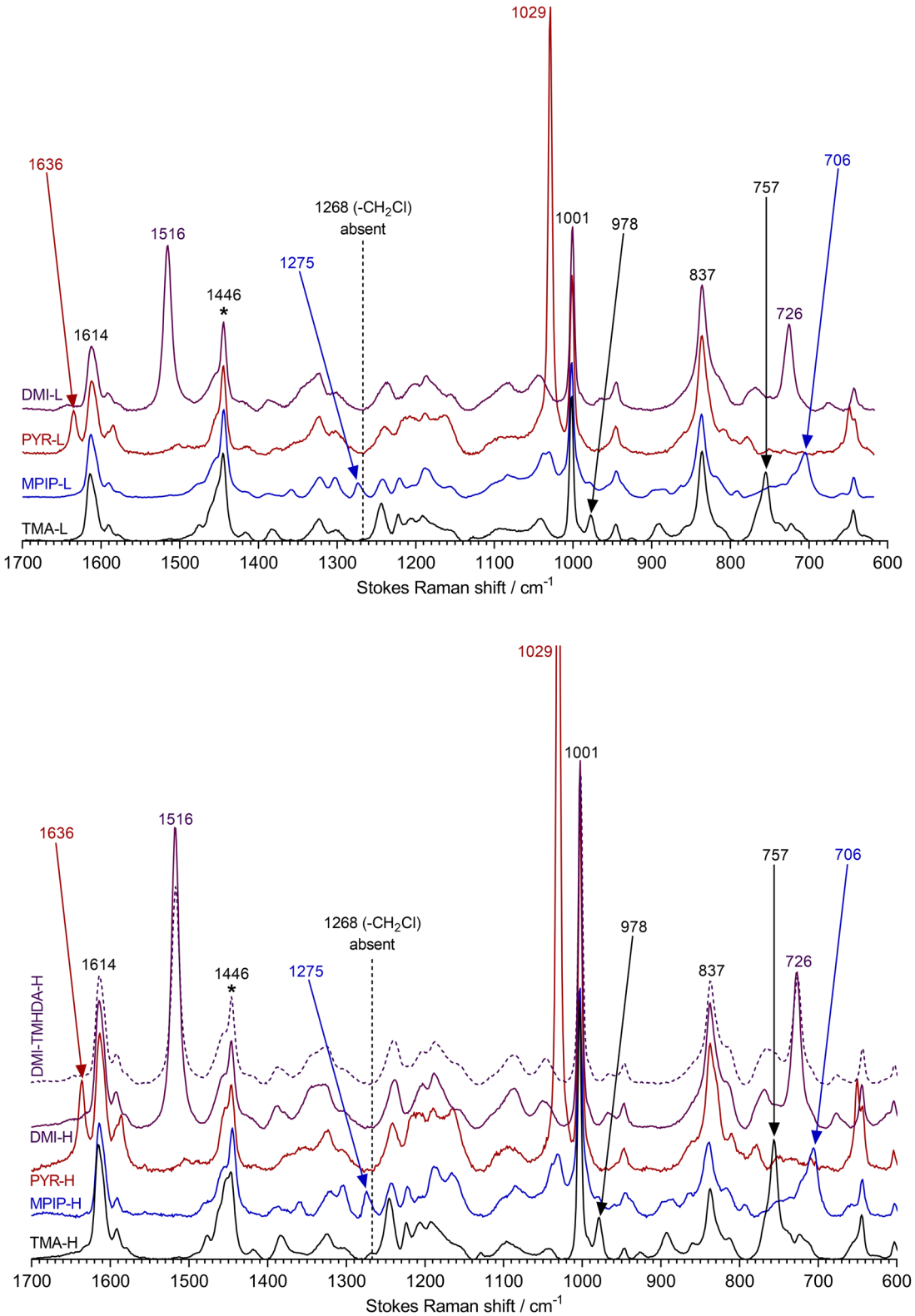

Fig. 1 The Raman spectra (785 nm excitation laser) of the low IEC (top) and high IEC (bottom) RG-AEMs synthesised. Each spectrum is the average of n = 10 spectra across both surfaces for each AEM and are normalised to the intensity of the 1446 cm^{-1} band to aid visual comparison (kept to same intensity in all spectra for ease of comparison of the low and high IEC RG-AEMs, hence the clipping of the intense 1029 cm^{-1} band in the bottom panel). Key bands are indicated and discussed in the main text.

Reflex Raman Microscope (Renishaw, UK) using a 785 nm near IR excitation laser and a 50× objective (NA = 0.5, *ca.* 2 μm laser Airy spot size). Across both surfaces of each RG-AEM sample, n = 10 spectra in total were recorded on random spots (n = 5 on

each side). For each RG-AEM, all individual spectra were baseline corrected before being normalised to the intensity of the 1446 cm^{-1} band (CH_2 scissor mode of the ETFE substrate) and averaged (arithmetic mean) using SpectraGryph v. 1.2 optical spectroscopy software. The spectrum of DMI-TMHDA-H (dashed) was shifted +3.5 cm^{-1} to correct for a Raman shift calibration error during data collection (as detected by the misalignment of the intense aromatic band at 1001 cm^{-1}). The raw spectral files (Renishaw.wdf format) and the data used to plot Fig. 1 (Microsoft Excel.xlsx format) can be downloaded from DOI: **https://doi.org/10.6084/m9.figshare.22128719** (CC-BY licence).

Physical property measurement

The measurement of the following key RG-AEM properties (presented in Table 2) were conducted using the exact same methods described previously[3] [and will not be repeated here]:

1. The ion-exchange capacities (IEC_{quat} for all RG-AEMs and also IEC_{total} for the TMHDA-crosslinked RG-AEM, see Scheme 1 for the rationale for this), which give the amount (mmol) of positively charged cationic groups normalised to the mass of the dehydrated RG-AEM sample in the Cl^- form;

2. The thickness (though-plane) swelling (TPS), which is the percentage thickness increase of an RG-AEM sample on hydration normalised to the thickness of the dehydrated sample;

3. The gravimetric water uptakes (WU), which is the percentage mass increase of an RG-AEM sample on hydration normalised to the mass of the dehydrated sample;

4. The $\lambda(H_2O)$ values, which is the number of H_2O molecules per cationic site in the fully hydrated RG-AEM samples;

5. The 4-probe in-plane Cl^- conductivities (σ_{Cl^-}) of the RG-AEM samples when immersed in UPW at 25 ± 1 °C;

The apparent permselectivities (α) of the RG-AEM samples is the property that needs to be specifically enhanced in RG-AEMs for use in (reverse)electrodialysis application. A home-made Perspex cell was used with two electrolyte compartments, separated by a membrane holder, and with two fixed distance holes for reference electrodes (RE). Two double junction Ag/AgCl REs (Metrohm) were immersed in each electrolyte compartment of the cell to measure the potential difference across the RG-AEM samples using Autolab PGSTAT302N potentiostat (Metrohm). During permselectivity measurement, two aqueous NaCl solutions with 0.1 mol dm^{-3} and 0.5 mol dm^{-3} concentrations were circulated (single pass) through each compartment, respectively, using peristaltic pumps (Cole-Parmer, Masterflex L/S Digital drive).

Apparent permselectivities (α) were calculated using eqn (1) (repeated with n = 3 samples of each RG-AEM):[3,9]

$$\alpha\ (\%) = 100\% \times \frac{E_M}{E_T} = 100\% \times \frac{E - E_{offset}}{E_T} \qquad (1)$$

where E_M is the membrane potential, E is the measured potential difference, E_{offset} is potential difference between two reference electrodes when no RG-AEM was in place and aqueous NaCl (0.5 mol dm^{-3}) solutions was circulated in both compartments, and E_T is the theoretical Nernstian potential calculated for a 100% permselective membrane (37.9 mV).

Results and discussion

Raman characterisation

The Raman spectra of the different intermediate ETFE-*g*-poly(VBC) membranes used in this study contained superpositions of the spectrum of ETFE and the spectrum of poly(vinylbenzyl chloride) homopolymer as previously reported [data for an example spectrum of ETFE-*g*-poly(VBC) with a DoG = 46% can be found at DOI: **https://doi.org/10.6084/m9.figshare.22128719**].[3,7] Key diagnostic peaks (within *ca.* 2 cm^{-1}) include: an ETFE CH_2 scissor mode band (1446 cm^{-1}), an ETFE CF_2 band (837 cm^{-1}), an aromatic ring quadrant mode for the benzene rings in the grafted chains (1614 cm^{-1}), a breathing mode of *meta*-disubstituted benzene rings (1001 cm^{-1}), and a band due to the $–CH_2Cl$ groups in the grafted chains (1268 cm^{-1}).

All spectra of the low IEC RG-AEMs (Fig. 1 top) confirmed successful reaction of the ETFE-*g*-poly(VBC) with the quaternising agents due to the general absence of the 1268 cm^{-1} band. The average spectrum of TMA-L contains the expected bands at 757 and 978 cm^{-1},[5,7] while that of MPIP-L contains diagnostic bands at 706 and 1275 cm^{-1},[3,5] PYR-L contains intense bands at 1029 and 1636 cm^{-1},[8] and DMI-L contains intense bands at 726 and 1516 cm^{-1}.[6]

The high IEC variants (Fig. 1 bottom) show the same evidence of complete reactions with the quaternising agents and the introduction of TMA, MPIP, PYR, and DMI groups. However, the bands for the cationic headgroups are more intense compared to the bands derived from the ETFE-substrate (*cf.* the low IEC variants), consistent with the higher IECs.

The Raman characterisation of the incorporation of crosslinking into DMI-TMHDA-H is less clear as the key but weak diagnostic Raman bands for the incorporated TMHDA groups is at *ca.* 757 cm^{-1},[3] which overlaps with an adjacent 786 cm^{-1} DMI-derived band. However, TMHDA incorporation and crosslinking can be inferred from the combination of the following evidence:

1. The average spectrum of DMI-TMHDA-H, compared to DMI-H, contains smaller relative intensities of the DMI-derived bands at 726 and 1516 cm^{-1} (*cf.* the ETFE 1446 cm^{-1} band used to normalise the spectra), despite both RG-AEMs having comparable IECs;

2. A small enhancement of Raman scattering intensity at 757 cm^{-1} in the spectrum of DMI-TMHDA-H;

3. The dramatically reduced TPS and water contents (Table 2, *vide supra*) provides clear evidence of crosslinking;

4. The IEC_{total}/IEC_{quat} ratio of 1.09 obtained with DMI-TMHDA-H indicates a mixture of crosslinked and non-crosslinked TMHDA-based groups are present in the RG-AEM (Table 2 and Scheme 1).[3] However, the presence of tertiary amine groups (leading to $IEC_{total} > IEC_{quat}$) does provide further evidence of TMHDA incorporation.

The physical properties of the RG-AEMs

Regarding the key property apparent permselectivity (α), the non-crosslinked RG-AEMs all have very low α values of < 70% (Table 2), with the MPIP headgroup performing worse than the

TMA headgroup (for comparable IEC RG-AEMs), which all confirms previous observations.[3] The high IEC variants have lower permselectivity values compared to the low IEC variants, and this is due to the higher levels of swelling in water (*vide infra*). This is as expected with dilution of the cationic groups in the high IEC RG-AEMs lowering the fixed charge densities (C_{fix}), which leads to lower permselectivities.[1,10]

Looking at the relationship between α and room temperature Cl^- conductivities (σ_{Cl^-}) (Fig. 2 left), the aromatic DMI headgroup seems to provide the best α values without excessive losses of conductivity compared to the other headgroups (including with the other aromatic headgroup, PYR, which yields the highest conductivities but with poorer α values). Ji *et al.*,[4] found that the nature of the fixed charged [cationic] group had only a minor influence on apparent permselectivity of their AEMs in aqueous NaCl; however, they only studied crosslinked, low IEC (1.2 mmol g^{-1}) AEMs containing either TMA and DMI groups. Our study, with a wider range of headgroups and IECs and a different AEM architecture, shows that the headgroup can influence permselectivities. Despite the different headgroups affecting the α–σ_{Cl^-} balance of the RG-AEMs, no clear trend is apparent, with headgroups behaving differently for the low and high IEC series.

However, looking at the trends between α values and water contents, either WU or $\lambda(H_2O)$, a clearer picture emerges. It is

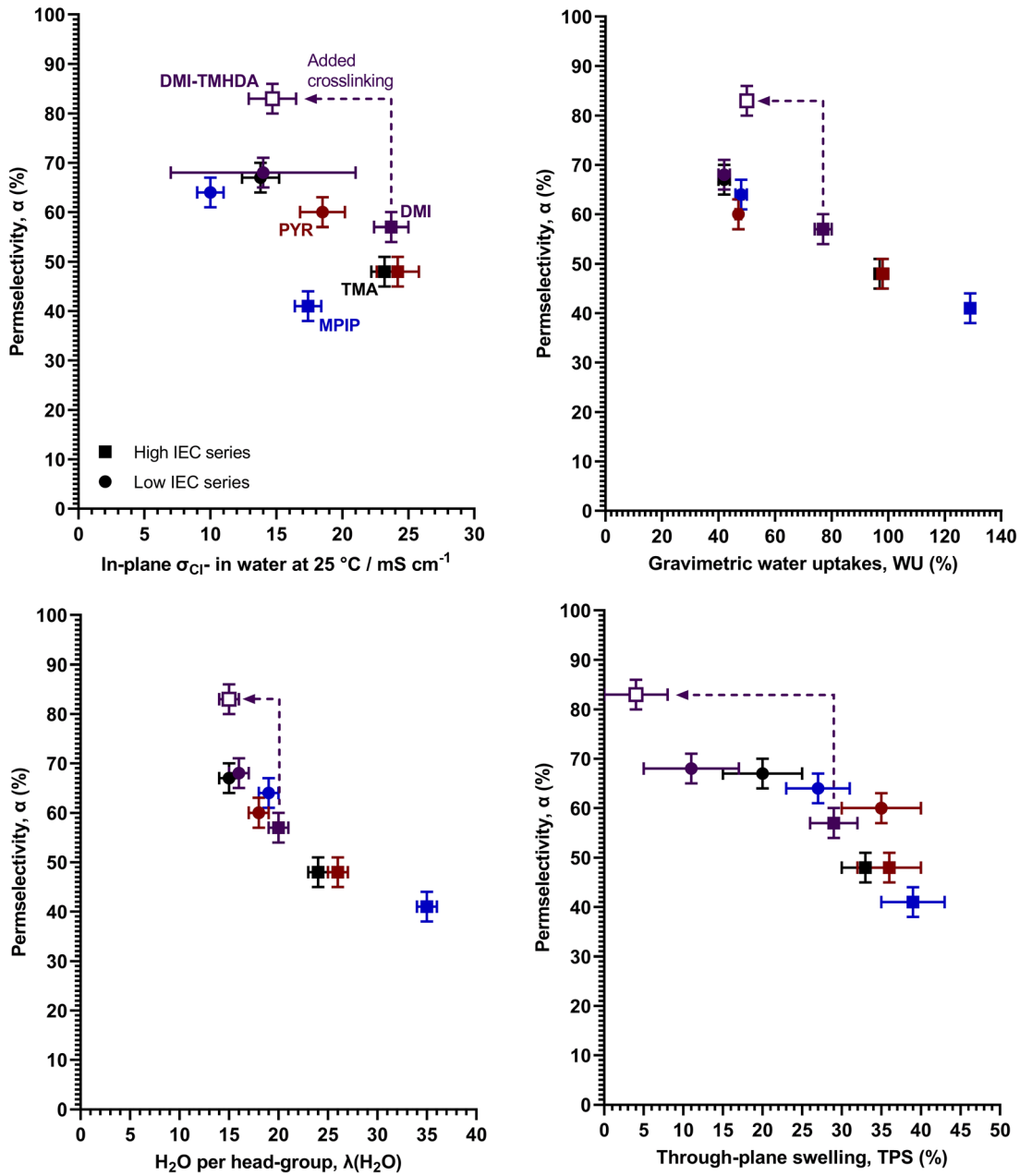

Fig. 2 The variations in apparent permselectivities with Cl^- conductivities (top left), gravimetric water uptakes (top right), $\lambda(H_2O)$ (bottom left), and through-plane (thickness) swelling (bottom right) for all the RG-AEMs in this study.

now apparent that the headgroups are affecting the water contents and the most important trend is between water contents and α values (Fig. 2), with low water contents leading to higher α values. This also explains why the high IEC RG-AEMs have lower α values (*cf.* low IEC RG-AEMs). Furthermore, there is also a reasonable correlation between α values and TPS (thickness swelling, correlation also shown in Fig. 2). For both IEC series, the DMI RG-AEMs are amongst the lowest water contents (and the lowest swelling) examples. The raised α values for DMI-L and DMI-H again relate to the less diluted ion-exchange sites and higher C_{fix}.[1,10] Additionally, MPIP-L and PYR-L provide the ability to compare two RG-AEMs with the same WU but different TPS values, where PYR-L swells a little bit more and consequently yields a slightly lower mean α value (Table 2).

To reconfirm the previous finding that TMHDA-based crosslinking can improve α,[3] a high IEC DMI-based RG-AEM was fabricated with added TMHDA in the quaternisation mixture (DMI-TMHDA-H). A high IEC was chosen as adding TMHDA into the RG-AEMs also leads to a lowering of conductivity and the higher IEC RG-AEMs had higher conductivities to begin with (*cf.* the low IEC series). The crosslinked DMI-TMHDA-H RG-AEM clearly had greatly improved α (the only RG-AEM in this study to achieve $>80\%$) compared to a similar conductivity RG-AEMs, whilst being the only RG-AEM to clearly break from the α – water content trend (Fig. 2). This shows that TMHDA-crosslinking can be as effective with aromatic headgroup RG-AEMs as it was with the previously reported aliphatic MPIP-based RG-AEMs.[3]

Conclusions

A series of non-crosslinked radiation-grafted anion-exchange membranes (RG-AEM) containing different headgroup chemistries, with either low or high ion-exchange capacities (IEC), were fabricated. Lower IEC variants led to higher apparent permselectivities, but at the expense of lower ionic conductivities. The headgroup chemistry of RG-AEMs (with comparable IECs) can also affect the balance between permselectivity and Cl^- conductivity. However, this is primarily due to the different headgroups yielding RG-AEMs with varying water contents. The RG-AEMs with the lowest water contents led to the highest permselectivities (as lower levels of swelling will lead to higher fixed charge densities). The non-crosslinked RG-AEMs containing 1-benzyl-2,3-dimethylimidazolium (DMI) headgroups contained some of the lowest water contents and therefore exhibited the highest permselectivities (at each IEC level), while retaining reasonable Cl^- conductivities.

Addition of ionic crosslinking (*N*,*N*,*N*′,*N*′-tetramethylhexane-1,6-diamine (TMHDA) incorporation) to a high IEC DMI-type RG-AEM disrupted the permselectivity–water content trend (seen with the non-crosslinked variants) and yielded a disproportionately high permselectivity. These findings suggest that high IEC AEMs (not only RG-types) that contain ionic crosslinks and imidazolium-based headgroups are worthy of further study for application in (reverse)electrodialysis applications. A future study should therefore compare RG-AEMs with non-RG-types containing imidazolium-TMHDA formulations, including their effect on *in situ* (reverse)electrodialysis cell performances.

Conflicts of interest

There are no conflicts to declare.

Acknowledgements

This study was funded by the UK's Engineering and Physical Sciences Research Council (EPSRC grant EP/R044163/1, REDAEM project). The Raman microscope was funded by EPSRC grant EP/M022749/1. We thank Dr Friedrich Menges for granting us a free use licence to SpectraGryph (**https://www.effemm2.de/spectragryph/index.html**).

References

1 M. N. Z. Abidin, M. M. Nasef and J. Veerman, *Desalination*, 2022, **537**, 115854; J. Jang, Y. Kang, J.-H. Han, K. Jang, C.-M. Kim and I. S. Kim, *Desalination*, 2020, **491**, 114540; R. A. Tufa, S. Pawlowski, J. Veerman, K. Bouzek, E. Fontananova, G. di Profio, S. Velizarov, J. G. Crespo, K. Nijmeijer and E. Curcio, *Appl. Energy*, 2018, **225**, 290; B. E. Logan and M. Elimelech, *Nature*, 2012, **488**, 313.
2 H. Fan and N. Y. Yip, *J. Membr. Sci.*, 2019, **573**, 668; G. M. Geise, M. A. Hickner and B. E. Logan, *ACS Appl. Mater. Interfaces*, 2013, **5**, 10294.
3 R. Bance-Soualhi, M. Choolaei, S. A. Franklin, T. R. Willson, J. Lee, D. K. Whelligan, C. Crean and J. R. Varcoe, *J. Mater. Chem. A*, 2021, **9**, 22025.
4 Y. Ji, H. Luo and G. M. Geise, *Phys. Chem. Chem. Phys.*, 2020, **22**, 7283.
5 J. Ponce-González, D. K. Whelligan, L. Wang, R. Bance-Soualhi, Y. Wang, Y. Peng, H. Peng, D. C. Apperley, H. N. Sarode, T. P. Pandey, A. G. Divekar, S. Seifert, A. M. Herring, L. Zhuang and J. R. Varcoe, *Energy Environ. Sci.*, 2016, **9**, 3724.
6 O. M. M. Page, S. D. Poynton, S. Murphy, A. Ong, D. M. Hillman, C. A. Hancock, M. G. Hale, D. C. Apperley and J. R. Varcoe, *RSC Adv.*, 2013, **3**, 579.
7 L. Wang, E. Maggliocca, E. L. Cunningham, W. E. Mustain, S. D. Poynton, R. Escudero-Cid, M. M. Nasef, J. Ponce-González, R. Bance-Soualhi, R. C. T. Slade, D. K. Whelligan and J. R. Varcoe, *Green Chem.*, 2017, **19**, 831.
8 K. Wieszczycka, K. Filipowiak, A. Lewandowska, A. Marcinkowska and M. Nowicki, *Molecules*, 2022, **27**, 1723.
9 J. G. Hong and T. W. Park, *J. Electroanal. Chem.*, 2018, **818**, 134; P. Długołęcki, K. Nymeijer, S. Metz and M. Wessling, *J. Membr. Sci.*, 2008, **319**, 214.
10 A. S. Gangrade, S. Cassegrain, P. C. Ghosh and S. Holdcroft, *J. Membr. Sci.*, 2022, **641**, 119917.